American Journal of Pathology, Vol. 166, No. 1, January 2005

Cardiovascular, Pulmonary and Renal Pathology

Triglycidylamine Crosslinking of Porcine Aortic Valve Cusps or Bovine Pericardium Results in Improved Biocompatibility, Biomechanics, and Calcification Resistance

Chemical and Biological Mechanisms

Jeanne M. Connolly,* Ivan Alferiev,* Jocelyn N. Clark-Gruel, Naomi Eidelman,† Michael Sacks,‡ Elizabeth Palmatory,* Allyson Kronsteiner,* Suzanne DeFelice,* Jie Xu,* Rachit Ohri,* Navneet Narula,§ Narendra Vyavahare,* and Robert J. Levy*

From the Division of Cardiology, The Children's Hospital of Philadelphia, Philadelphia Pennsylvania; the Paffenbarger Research Center,† American Dental Association Foundation, National Institute of Standards and Technology, Gaithersburg, Maryland; the Department of Bioengineering,‡ University of Pittsburgh, Pittsburgh, Pennsylvania; and the Department of Pathology,§ University of Pennsylvania School of Medicine, Philadelphia, Pennsylvania*

We investigated a novel polyepoxide crosslinker that was hypothesized to confer both material stabilization and calcification resistance when used to prepare bioprosthetic heart valves. Triglycidylamine (TGA) was synthesized via reacting epichlorhydrin and NH_3. TGA was used to crosslink porcine aortic cusps, bovine pericardium, and type I collagen. Control materials were crosslinked with glutaraldehyde (Glut). TGA-pretreated materials had shrink temperatures comparable to Glut fixation. However, TGA crosslinking conferred significantly greater collagenase resistance than Glut pretreatment, and significantly improved biomechanical compliance. Sheep aortic valve interstitial cells grown on TGA-pretreated collagen did not calcify, whereas sheep aortic valve interstitial cells grown on control substrates calcified extensively. Rat subdermal implants (porcine aortic cusps/bovine pericardium) pretreated with TGA demonstrated significantly less calcification than Glut pretreated implants. Investigations of extracellular matrix proteins associated with calcification, matrix metalloproteinases (MMPs) 2 and 9, tenascin-C, and osteopontin, revealed that MMP-9 and tenascin-C demonstrated reduced expression both *in vitro* and *in vivo* with TGA crosslinking compared to controls, whereas osteopontin and MMP-2 expression were not affected. TGA pretreatment of heterograft biomaterials results in improved stability compared to Glut, confers biomechanical properties superior to Glut crosslinking, and demonstrates significant calcification resistance. *(Am J Pathol 2005, 166:1–13)*

Heterograft valve bioprostheses fabricated from either glutaraldehyde (Glut)-fixed porcine aortic valves or bovine pericardium have been extensively used throughout the past 30 years in cardiac valve replacement surgery for valvular disease.[1] Although these bioprostheses have less risk of thromboembolic complications than mechanical heart valve prostheses, their clinical course is frequently complicated by pathological calcification of the valve cusps. One of the mechanistic factors responsible for bioprosthetic cuspal calcification is Glut fixation. Glut pretreatment has been demonstrated to predispose bioprosthetic implants to calcification because of several important mechanistic factors.[2,3] For instance, Schiff bases formed as a result of Glut crosslinking are unsta-

Supported by the National Institutes of Health (grants HL74731 and HL38118 to R.J.L., HL07915 to J.N.C.), the William J. Rashkind Endowment of the Children's Hospital of Philadelphia (to R.J.L.), the National Institutes of Standards and Technology (to N.E.), and the American Dental Association Foundation (to N.E.).

Accepted for publication September 14, 2004.

Address reprint requests to Robert J. Levy, M.D., Abramson Research Center 702, Children's Hospital of Philadelphia, 3615 Civic Center Blvd., Philadelphia, PA 19104. E-mail: levyr@email.chop.edu.

ble, leading to the leaching of Glut with subsequent cytotoxic and inflammatory activity that can contribute to calcification.[4,5] Glut fixation of heterograft materials has also been demonstrated to be associated with stabilization of calcifiable cellular structures and extracellular matrix components, such as collagen, that are involved in the mechanisms of bioprosthetic calcification.[2] The present studies focused on an epoxy crosslinking strategy, seeking a crosslinking agent that would form irreversible bonds with structural proteins, and at the same time favorably alter collagen structure to mitigate pathological calcification. Polyepoxy crosslinkers (that were not tertiary-glycidyl amines) have been previously studied for fixation of bioprosthetic heart valves, with in general unsatisfactory results.[6–9] This may have been because of the relatively poor water solubility of the polyepoxys studied, chemical heterogeneity, and contamination with residual reactants, such as organo-chlorides.[6–9] The present studies investigated triglycidylamine (TGA), a highly polar, water-soluble polyepoxy-crosslinking agent. We investigated the hypothesis that TGA confers calcification resistance because of its unique reactions with extracellular matrix (ECM) proteins, thereby favorably altering the mechanistic events associated with pathological mineralization.

Our experiments pursued the following goals: 1) to synthesize, purify, and chemically characterize TGA; 2) to investigate TGA's effectiveness as a crosslinking agent; 3) using sheep aortic valve interstitial cells (SAVICs) *in vitro*, to explore the effects of TGA crosslinking of type I collagen cell culture substrates on cellular viability and cell-mediated calcification, and the effects of TGA crosslinking on ECM-related calcification mechanisms; and 4) to investigate *in vivo*, using rat subdermal implants, ECM-related mechanisms associated with TGA crosslinking inhibiting the calcification of bioprosthetic cusp implants.

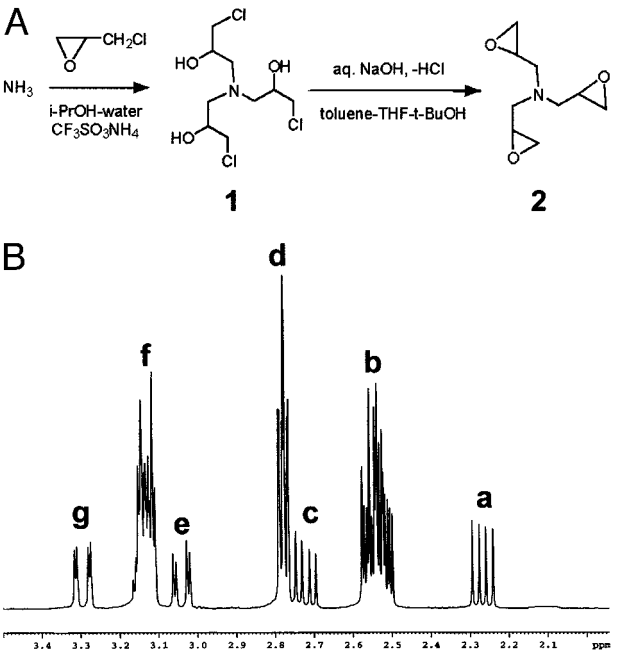

Figure 1. Preparation and characterization of TGA. **A:** To produce TGA (2), ammonia was reacted with an excess of epichlorohydrin in aqueous isopropanol in the presence of ammonium triflate as a catalyst to give Tris-(3-chloro-2-hydroxypropyl)amine. (1) The latter was dehydrochlorinated to 2 in a mixture of solvents (toluene, tetrahydrofuran, and tert-butanol) by addition of concentrated aqueous NaOH. **B:** ^{1}H-NMR ($CDCl_3$) showing diasteriomers 1 and 2 of TGA; δ 2.25 (a) (dd, 14, 7 Hz, 3H of minor isomer, diastereotopic CH_2N), 2.49 to 2.57 (b) (m, 3H of both isomers, oxirane CH_2 + 2H of principal diastereomer, diastereotopic CH_2N with predominant chirality), 2.72 (c) (dd, 14, 7 Hz, 1H of principal isomer, diastereotopic CH_2N with subdominant chirality), 2.76 to 2.81 (d) (m, 3H of both isomers, oxirane CH_2), 3.04 (e) (dd, 14, 3 Hz, 1H of principal isomer, diastereotopic CH_2N with subdominant chirality), 3.11 to 3.17 (f) (m, 3H of both isomers, CH + 2H of principal diastereomer, diastereotopic CH_2N with predominant chirality), 3.30 (g) (dd, 14, 2 Hz, 3H of minor isomer, diastereotopic CH_2N).

Materials and Methods

Chemical Synthesis and Characterization

All chemicals were obtained reagent grade from Sigma-Aldrich Chemicals, St. Louis, MO. TGA (Figure 1A, schematic 2) was synthesized as follows. Aqueous ammonia was reacted with an excess of epichlorohydrin and catalytic amounts of ammonium triflate in isopropanol for 48 hours at 20 to 24°C, then for 3 hours at 30 to 35°C. The solvents were distilled off at 30 to 40°C and 15 to 20 mm Hg, the residual epichlorohydrin was removed by co-evaporations with a mixture of toluene and tert-butanol at the same vacuum and at 40 to 45°C. The resulting thick colorless syrup consisting mostly of Tris-(3-chloro-2-hydroxypropyl)amine (Figure 1A, schematic 1) was dissolved in a mixture of toluene, tetrahydrofuran, and tert-butanol. An excess of 50% aqueous NaOH solution was added at 18 to 22°C under vigorous stirring. In 2 hours the epoxy-ring closure was complete. Ice-cold water was added to dissolve the precipitate of NaCl and the organic layer was separated and then dried overnight over anhydrous potassium carbonate at 4°C. The desiccant was filtered off, the filtrate was vacuum-concentrated at vacuum to 1 mm Hg and temperature up to 50°C. The residue was vacuum-distilled at 0.08 to 0.10 mm Hg to give pure TGA (Figure 1A, schematic 2) in a 72% yield as a viscous liquid, Bp = 80 to 85°C, slowly solidifying at −15°C, and then remaining solid at room temperature. The product was characterized using TLC (silica gel, $CHCl_3$-MeOH, 92:8, spot detection in I_2-chamber), which showed a single spot with an R_f = 0.7, and by ^{1}H-NMR (Bruker Advance DMX 400 Spectrometer, Bruker Optics, Inc., Billerica, MA 400MHz, $CDCl_3$) (Figure 1B).

Implant Preparation

Fresh porcine aortic valve leaflets and bovine pericardium were shipped overnight on ice from St. Jude Medical (Minneapolis, MN). On arrival, all were rinsed extensively in sterile normal saline solution, and fixed with either Glut or with TGA as follows. Glut-fixed tissues were prepared as previously published[10] with 0.6% Glut (EM grade; Polysciences, Inc., Warrington, PA) in 50 mmol/L HEPES/0.9% NaCl buffer, pH 7.4, at room temperature for 7 days with one change, then stored in 0.2% buffered Glut at room temperature until use. Tissues fixed with

TGA were treated with 100 mmol/L TGA in borate mannitol buffer (25 mmol/L sodium tetraborate decahydrate, pH 7.4) at room temperature with daily changes of the TGA solution for 7 days. Before implantation, all materials were rinsed three times for 1 hour in an excess of sterile normal saline.

Differential Scanning Calorimetry Analysis

Porcine aortic valve cusps and bovine pericardium were crosslinked with Glut or TGA as described above. Sample sets were removed at designated time points, rinsed in sterile saline, and shrink temperature (Ts) determined using a DSC7 (Perkin-Elmer, Inc., Wilson, CT) with temperature ramping from 60°C to 100°C. Analyses were typically performed in replicates of three.

Fourier Transform Infrared Spectroscopy (FTIR) Analysis

Analyses were performed on untreated or Glut- or TGA-treated porcine aortic valve cusps and on bovine pericardium likewise prepared with the 7-day room temperature crosslinking protocols described above. Untreated, Glut-, and TGA-crosslinked porcine aortic valve leaflets and bovine pericardium were embedded on dry-ice in OCT (Sakura USA, Torrance, CA), and cryosectioned (4 μm thick). The sections were placed on reflective glass slides (Kevley Technologies, Chesterland, OH) for reflectance-transmission FTIR microspectroscopy measurements (FTIR-RTM),[11] The FTIR-RTM analyses were performed using a Nicolet Magna-IR 550 FTIR spectrophotometer (Nicolet Instrumentations Inc., Madison, WI) interfaced with a Nic-Plan IR microscope (Spectra-Tech, Inc., Shelton, CT). The spectral point-by-point mapping of the porcine aortic valve cusp sections was performed in a grid pattern with the use of the computer-controlled microscope stage and Atlus (Nicolet) mapping software. The sections were mapped with a spatial resolution of 200 μm (total of 504 to 3360 spectra per map) with 32 to 128 scans per acquired spectrum in the 650 cm^{-1} to 4000 cm^{-1} region and 8 cm^{-1} resolution. The FTIR spectra were proportioned against the background of the reflective slide. Six spectra were extracted from each map from locations spread across the section. The spectra were deconvoluted in the 1800 to 1300 cm^{-1} regions, and their peaks were identified by the Omnic software (Nicolet). In addition, each set of six spectra was processed to an averaged spectrum by the Ominc software. These spectra were also deconvoluted and their peaks were identified. Ten spectra were acquired from various spots (200 μm $\times$ 200 μm) of four sections from each treatment group of the bovine pericardium or valves. The spectra were obtained with 64 scans in the 650 cm^{-1} to 4000 cm^{-1} region and 8 cm^{-1} resolution. Each set of 10 spectra was signal-averaged and deconvoluted as described above. In addition, type I collagen gels were formulated on reflective slides as described for cell culture experiments (protocol shown below) and subjected to overnight incubation with either TGA, Glut, or buffer before FTIR analysis, using the Nicolet Protégé 460 FTIR spectrophotometer equipped with a Nicolet InspectIR Microscope attachment. Fifty scans were obtained at a resolution of 4 cm^{-1}, and the spectra were deconvoluted with Omnic software in the 1800 to 1300 cm^{-1} regions after subtraction of a water reference.

Collagenase Digestibility

Porcine aortic valve leaflets were crosslinked for 7 days as above at room temperature in either Glut or TGA. After crosslinking, both sets were rinsed exhaustively with sterile saline. Samples were placed into individual tared microfuge tubes, lyophilized, and weighed. Samples were digested for 1 hour at 37°C using a solution of 0.1% type I Collagenase (Sigma C-9722 IA-S) in phosphate-buffered saline containing 0.1% bovine serum albumin (Sigma). After 1 hour of digestion, samples were chilled to 4°C, pelleted by centrifugation at 14,000 rpm, and washed with sterile saline. Resulting washed pellets were lyophilized and weighed. Data were calculated as a percent loss from the original dry porcine aortic valve leaflet weight.

Compliance and Stretch

Structurally consistent biaxial specimens from the chemically modified bovine pericardium were selected using small angle light scattering, and biaxial mechanical testing was performed as previously described.[12,13] Briefly, testing was performed with the specimen immersed in phosphate-buffered normal saline (pH 7.4) at room temperature. A stress controlled test protocol was used, wherein the ratio of the normal Lagrangian stresses (force/original cross-sectional area) was kept constant.

Flexure response and rigidity were tested as previously described,[14,15] using 10 TGA and 10 Glut specimens that were selectively aligned along the preferred (PD) and cross-preferred (XD) collagen fiber direction of specimens originally used for the nondestructive biaxial mechanical testing. To compute the effective modulus (E) of the tissue specimen we used the generalized Bernoulli-Euler moment-curvature relation for beams undergoing large displacements:

$$M = EI\Delta\kappa$$

where $\Delta\kappa$ represents the change in specimen curvature from the reference state, computed as the difference between the initial specimen curvature and the deformed curvature; I is the second moment of inertia computed from the specimen geometry, and M is the applied bending moment. M is determined from the applied loads and specimen geometry, I from the width and thickness of the specimen ($I = wt^3/12$, w = specimen width, t = specimen thickness). The equation is analogous to Hooke's law (ie, $\sigma = E\,\epsilon$, where σ is stress, E is Young's modulus, and ϵ is the strain) for a specimen subjected to flexure as opposed to uniaxial tension. Note that EI is known as the flexural rigidity, representing the effective stiffness of the specimen.

Cells and Cell Culture

Rat arterial smooth muscle (A10) and human umbilical vein endothelial cell (HUVEC) cell lines were obtained from American Type Culture Collection (Rockville, MD). SAVICs were isolated as previously described[16] and used between passages 2 and 10. Cells were routinely cultured in M199 (Life Technologies, Inc., Grand Island, NY) supplemented with 10% fetal bovine serum (Hyclone, Logan UT) and penicillin/streptomycin (Life Technologies, Inc.). In experiments involving the study of matrix metalloproteinases (MMPs) and quantitation of calcification, serum content was reduced to 0.5% fetal bovine serum, and 10 mmol/L glycerophosphate and 1.5 mmol/L $CaCl_2$ were added plus or minus 10 ng/ml of transforming growth factor (TGF)-β1 (R&D Systems, Minneapolis, MN), as previously described.[17] Collagen culture substrates were prepared in tissue culture plates by gelation of neutralized native type I collagen (Cohesion Technologies, Inc., Palo Alto, CA) according to manufacturer's directions. The collagen volume of each cell culture plate's collagen coating was normalized to 0.158 ml/cm^2 of growth surface area, and stored under normal saline at 37°C until use. For TGA collagen, after gelation of collagen as just described, an equal volume of 100 mmol/L TGA in borate mannitol buffer was incubated overnight at 37°C. The plates were then washed three times with sterile normal saline, and residual epoxy groups neutralized by subsequent overnight incubation at 37°C with 0.1 mol/L sodium thiosulfate in borate mannitol buffer. After washing three times again with sterile normal saline, plates were stored under normal saline until use. Cells were plated at a density normalized to 5.3×10^4 cells/cm^2.

Biocompatibility and Cell Viability

All experiments were performed in triplicate cultures. Cells were plated as above in reduced serum (2% fetal bovine serum) for 24 hours before assessment of their condition. Biocompatibility was qualitatively assessed using the Live/Dead assay (Molecular Probes, Eugene, OR) per the manufacturer's directions, in which viability is indicated by enzymatic metabolism of calcein (green fluorescence) versus retention of EthD-1 by dead cells (red fluorescence).

Calcification in Cell Culture

Cells (SAVICs) were qualitatively assessed for calcification by alizarin red staining as previously described,[17,18] and quantitatively in parallel cultures by a modification of the *o*-cresolphthalein complexone method described by Wada and colleagues.[19] Briefly, at the end of each experiment, cultures were rinsed with saline, followed by decalcification with 0.6 N HCl for 24 hours. The calcium content of the HCl supernatant was determined by addition of 2 ml of color reagent [160 mmol/L *o*-cresolphthalein complexone (Sigma), 7 mmol/L 8-hydroxy-quinoline (Sigma) in 0.72 N HCl] to 0.100 ml of sample, standard or blank. The calcium concentration was determined by absorbance measurements at 540 nm on a microplate reader (Spectra Max 190; Molecular Devices, Sunnyvale, CA) using a calcium standard curve, and subtracting cell-free culture supernatant results as background controls. Results were normalized to cellular protein and reported as μmol Ca/mg protein. All experiments were performed in triplicate cultures.

Western Blots

Western blots were performed on SAVIC lysates according to established procedures using 10% sodium dodecyl sulfate-polyacrylamide gel electrophoresis under denaturing conditions. Cells were harvested from either collagen or TGA-collagen cultures by incubation at 37°C with 1 mg/ml type II collagenase (Sigma), followed by very gentle scraping to exclude substrate in the harvest. Lysates were prepared using RIPA buffer containing Complete protease inhibitor cocktail (Roche Biochemical, Indianapolis, IN). The protein concentration was determined using the Micro BCA protein assay (Pierce, Rockford, IL). Membranes were probed with dilutions of either rabbit anti-chicken tenascin-C (TNC) (AB19013; Chemicon, Temecula, CA) or rabbit anti-human osteopontin (OPN) (LF-166; supplied by Dr. L. Fisher, National Institutes of Health, Bethesda, MD). After enhanced chemiluminescence development of the signal (Amersham, Piscataway, NJ), membranes were stripped and reprobed with mouse anti-ERK2 (sc-154; Santa Cruz Biotechnology, Santa Cruz, CA) to verify loading.

Cellular Digestion Resistance TGA-Crosslinked Collagen

SAVICs were cultured in six-well plates on either collagen or TGA-collagen as described above for 14 days. Medium was aspirated and substrate carefully removed from each well by scraping into tared microfuge tubes. After lyophilization, weights of each were determined and calculated as a percent weight lost compared to weights of triplicate parallel wells incubated in medium without cells for the same time period.

Zymography

Zymography was performed as previously described,[16] using 10% polyacrylamide gel electrophoresis precast zymograph gels (Bio-Rad, Richmond, CA). Conditioned medium was harvested by aspiration from SAVIC cultures, clarified by centrifugation, and concentrated 10-fold using Centricon YM-30 microconcentrators (Millipore). After protein determination using the Bradford dye based assay (Bio-Rad), zymography was performed using 10 μg of conditioned medium protein per lane.

Rat Subdermal Implants

Male (21 to 25 days old) Sprague-Dawley rats were subjected to subdermal implants of fixed heterograft materi-

als (prepared as described above) under general anesthesia (ketamine and xylazine) as previously published,[19] and as approved by the Institutional Committee for the Use and Care of Animals of The Children's Hospital of Philadelphia. The implants were either porcine aortic cusps or 1-cm^2 portions of bovine pericardium prepared as described above. For calcification studies, each individual animal was implanted with one porcine aortic cusp and one bovine pericardium specimen from each fixation group, in groups of 10 animals. Thus, there were two groups of 10 animals used for the calcification studies, with a separate group for each fixation condition of interest: Glut-fixed pericardium and Glut-fixed porcine aortic cusps; and TGA-fixed bovine pericardium, and TGA-fixed porcine aortic valve cusps. For RNA isolation and reverse transcriptase (RT)-polymerase chain reaction (PCR) studies (see below) groups of 10 animals with four implants per animal were used so that specimens could be pooled to obtain sufficient RNA. Only porcine aortic cusps were used for these studies, and thus two groups of 10 animals were used, TGA-fixed and Glut-fixed. In this RT-PCR experiment, an additional three animals per group were used for confirmatory morphology and confirmatory Ca analysis (data not shown).

Explant Investigations: Morphology and Ca Analyses by Atomic Absorption Spectroscopy

On animal sacrifice, explants were rinsed in sterile saline, and half of each either frozen in OCT compound or placed in 10% neutral buffered formalin for later histological processing, and half stored at 4°C for later processing for Ca analyses. Explanted samples for quantitative calcium analyses were processed by acid hydrolysis, and Ca content determined using a Perkin-Elmer model 2380 atomic absorption spectrometer (Perkin-Elmer, Inc.), as previously described.[10]

Histological Processing of Explants

Rat subdermal explants embedded in frozen OCT compound or paraffin were cut to 5-μm cross sections and stained with alizarin red[18] or with hematoxylin and eosin. Serial sections were also immunostained using peroxidase methodology for either TNC, MMP-9, or OPN using rabbit anti-chicken TNC (Chemicon), mouse anti-human MMP-9 (IM37L; Oncogene Science, Boston, MA), or rabbit anti-human OPN (LF-166; Dr. L. Fisher) as primary antibodies, respectively, and using standard avidin-biotin amplification (Vectastain ABC; Vector Laboratories, Burlingame, CA) according to manufacturer's directions. TNC immunostaining was developed with Vector Laboratories VIP Purple as the final chromogen, while MMP-9 and OPN were developed with diaminobenzidine (Vector Laboratories) as the final chromogen. Visual scoring of staining was performed in a blinded manner, assigning a numerical rating of 1 to 5 based on the following criterion: 1 = negative, 2 = rare detection, 3 = sparse but consistent, 4 = uniformly present, and 5 = intense and widespread staining. TNC staining was evaluated in at least three $\times$50 fields per slide in six or eight explants from TGA and Glut treatment groups, respectively, while MMP-9 was evaluated in at least three sections per animal explant, using three animals per group.

RNA Isolation and Real-Time PCR (RT-PCR) Analyses

Rat explant valve cusp specimens were immediately snap-frozen in liquid nitrogen and stored at −80°C until processed. Four explants from the same rat were pooled (as above) and pulverized under liquid nitrogen, and were extracted with TRIzol (Life Technologies, Rockville, MD) according to manufacturer's directions. Tissue extracts were further purified by DNAase treatment to remove genomic DNA, and the RNA concentration was quantified by absorbance at 260 nm. Integrity and concentration were verified by electrophoresis on a 1% SeaKem agarose gel and on a RNA 6000 LabChip on the Agilent 2100 Bioanalyzer (Agilent Technologies, Palo Alto, CA). Five samples per group (as above) yielded sufficient high-quality RNA for RT-PCR analysis. RNA was converted to single-strand cDNA using the Superscript II kit (Life Technologies, Inc.) using 500 ng of RNA from each sample. Primers designed specifically for rat MMP-9 and TNC were: TNC (188) forward primer, ATGTTGAATGGCGACAC and reverse primer, CGGTCTCCAAACCCAG, and MMP-9 (129) forward primer, ACAGCCTGTTTCTGGT and reverse primer GATGCTGGATGCCTTTTAT.

Gene-specific copy number standards for TNC and MMP-9 were produced from amplicons generated by RT-PCR using the respective above primers and rat explant cDNA. For TNC, an amplicon of 188 bp was excised from a 1% agarose gel, and extracted using QIAex II Gel extraction kit (Qiagen, Valencia, CA), whereas for MMP-9, the process was repeated, producing an amplicon of 129 bp. For each, a TOPO TA cloning kit (Invitrogen, Carlsbad, CA) was used with the pCR 2.1 A TOPO vector for cloning of the amplicons. A Qiagen Plasmid MAXI kit (Qiagen) was used to isolate plasmid DNAs. The DNA concentration of each prep was quantified by absorbance at 260 nm and copy number was determined by calculating the relative number of molecules/μl. Serial dilutions were made from each, checked for linearity, and stored in aliquots at −80°C.

Lightcycler analyses were optimized and performed for TNC according to the manufacturer's directions using 5 μl of cDNA per run in the Lightcycler system (Roche Diagnostics, Inc., Indianapolis IN) using the Roche Lightcycler FastStart DNA Master SYBR Green (3003230) reagent kit and each reaction was run for 45 cycles. Samples were run in parallel with positive controls consisting of a serially diluted standard curve ranging from 10^{10} to 10^1 copies, from specific high concentration stocks generated for TNC as described above. After completion of the Lightcycler reactions, melting curves were run to ensure that the signal produced was specific to the target sequence and then run on 1% SeaKem agarose gels with a 100-bp ladder to ensure correct amplicon size. Calcu-

lations of unknowns were performed according to standards generated by Lightcycler software.

For MMP-9 studies TaqMan analyses were optimized and performed according to the manufacturer's directions using 5 μl of cDNA per reaction in the ABI Prism 7000 sequence detection system (Roche Diagnostics, Inc.) and Applied Biosystems (Foster City, CA) SYBR green master mix. Samples were run for 40 cycles in parallel with gene-specific positive controls consisting of a serially diluted standard curve ranging from 10^{10} to 10^{1} copies. Dissociation curves were checked using ABI Prism 7000 SDS software to ensure that the signal produced was specific to target sequence, and data were exported to spreadsheets for calculation of the copy number in comparisons with standards.

Statistical Analysis

Data for all experiments were expressed as means ±SEM (SE). The significance of differences was assessed using Student's *t*-test or Mann-Whitney rank sum test for sample sets failing a normal distribution test, and was termed significant when $P \leq 0.05$.

Results

TGA Chemical and Material Characterization

Purified TGA (Figure 1A) was obtained by vacuum-distillation at 0.08 to 0.10 mm Hg yielding a viscous liquid, with a boiling point of 80 to 85°C, slowly solidifying at −15°C, and then remaining solid at room temperature. TLC revealed the preparation to be one pure spot, with an $R_f \sim 0.73$. Because of the presence of chiral glycidyl groups, TGA was found to be a nonseparable mixture of two diastereomers in a 3:1 ratio, that were easily distinguished using ^{1}H-NMR (Figure 1B). These are postulated to differ in configuration at the C2 chiral centers of the glycidyl groups (RRR and SSS for the minor isomer; RRS and SSR for the principal isomer). Such a suggestion is in agreement with hypothetical considerations, that allow only two variants of structure for the former diastereomer (RRR and SSS), whereas for the latter one six variants (RRS, RSR, SRR, SSR, SRS, and RSS) are possible. Peaks are identified in Figure 1B, showing diasteriomers 1 and 2 of TGA; ^{1}H-NMR ($CDCl_3$) δ 2.25 (Figure 1B, a) (dd, 14, 7 Hz, 3H of minor isomer, diastereotopic CH_2N), 2.49 to 2.57 (Figure 1B, b) (m, 3H of both isomers, oxirane CH_2 + 2H of principal diastereomer, diastereotopic CH_2N with predominant chirality), 2.72 (Figure 1B, c) (dd, 14, 7 Hz, 1H of principal isomer, diastereotopic CH_2N with subdominant chirality), 2.76 to 2.81 (Figure 1B, d) (m, 3H of both isomers, oxirane CH_2), 3.04 (Figure 1B, e) (dd, 14, 3 Hz, 1H of principal isomer, diastereotopic CH_2N with subdominant chirality), 3.11 to 3.17 (Figure 1B, f) (m, 3H of both isomers, CH + 2H of principal diastereomer, diastereotopic CH_2N with predominant chirality), 3.30 (Figure 1B, g) (dd, 14, 2 Hz, 3H of minor isomer, diastereotopic CH_2N).

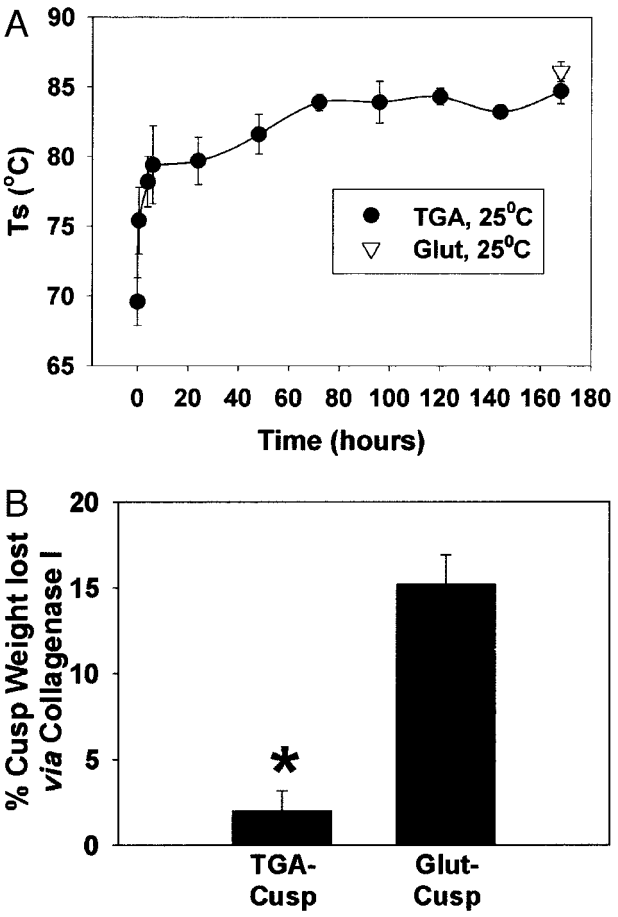

Figure 2. Crosslinking strength of TGA. **A:** Thermal denaturation temperatures (Ts) of porcine aortic cusps. Seven days of room temperature treatment with TGA results in Ts equal to that of the standard Glut crosslinking procedure. **B**: TGA crosslinked porcine aortic cusps are more resistant to collagenase digestion than are parallel gels crosslinked with Glut. (*, $P = 0.003$).

Differential Scanning Calorimetry and Collagenase Resistance

TGA crosslinking of porcine aortic valve cusps and bovine pericardium was assessed with differential scanning calorimetry in comparison studies with Glut-crosslinked porcine aortic valve cusps. TGA crosslinking at pH 7.4 and 25°C for 7 days attained the same Ts levels as observed with Glut fixation (Figure 2A). The Ts of TGA-treated bovine pericardium was 86.5 ± 0.2°C after 7 days, again comparing favorably to Glut-fixed pericardium (85.0 ± 0.1°C).

Furthermore, TGA-crosslinked porcine valve cusps were significantly more resistant to collagenase digestion than were Glut-fixed cusps (Figure 2B, $P = 0.003$). In parallel cell culture experiments, TGA-collagen proved resistant to SAVIC-mediated matrix digestion. After 14 days of culture, there was only a 6.3 ± 4.3% reduction in weight of the TGA-treated collagen culture substrate gel, compared to a 41.0 ± 9.9% reduction of noncrosslinked collagen ($P = 0.009$), a difference that may in part reflect a combination of down-regulation of cellular proteinases and TGA-crosslinked collagen demonstrating resistance

to digestion (see below). It should be noted that these studies were not performed on cells cultured on Glut-fixed collagen substrates because of the cytotoxicity noted when using Glut-fixed cell culture substrates (see below).

FTIR Spectroscopy

FTIR microspectroscopy studies were performed on purified native and TGA-treated collagen gels, on untreated, Glut-, and TGA-crosslinked porcine aortic valve leaflet sections, and on untreated, Glut-, and TGA-crosslinked bovine pericardial sections. FTIR surface analysis of type I collagen gels that had been crosslinked with TGA at 37°C overnight revealed a shift in peak height ratios in the amide I region at ~1650 to 1660 and 1630 cm^{-1}, compared to native collagen or Glut-fixed collagen (Figure 3A; c, a, and b, respectively). The FTIR-RTM spectra obtained from the sections of untreated, Glut-, and TGA-crosslinked porcine aortic valve leaflets (Figure 3B; a, b, and c, respectively) were relatively uniform throughout the cross sections (data not shown). The deconvoluted averaged spectra of six microscopic cross-sectional areas of the TGA-crosslinked aortic valve show also a decrease in the peak height ratio of amide I peaks appearing at ~1650 to 1660 and 1630 cm^{-1}. However, FTIR-RTM examination of untreated, Glut-, and TGA-crosslinked bovine pericardium sections showed uniformity across the sections and between different sections of the same group, but did not show any discernable peak rearrangements in the amides region (Figure 3C).

Biomechanical Testing

Small angle light scattering was used to orient bovine pericardial (BP) samples for testing to obtain appropriate orientation for this characteristically anisotropic biomaterial. Biaxial stress/strain studies demonstrated that TGA-pretreated bovine pericardium had significantly greater Lagrangian strain tolerance compared to Glut-pretreated pericardium (Figure 4A). These results were documented for both the preferred collagen fiber orientation as well as for the cross-fiber orientation. Overall TGA-pretreated pericardium was demonstrated to have superior compliance properties compared to Glut-fixed pericardium (Figure 4, A and B) with ~30% greater compliance demonstrated for TGA-pretreated pericardium versus Glut-fixed at 1 Mpa equibiaxial stress. The flexural rigidity (EI) of TGA-treated (BP) (11.21 mN-mm^2) was approximately one-half of the Glut-treated BP specimens (23.09 mN-mm^2) and was significantly different ($P = 0.002$). The tissue moduli E computed from the EI values were 281.82 kPa and 363.36 kPa for TGA- and Glut-treated bovine pericardium, respectively (Figure 4B), and these data were statistically significantly different ($P = 0.03$). Thus, it can be concluded that TGA-treated tissue is more compliant than Glut-treated.

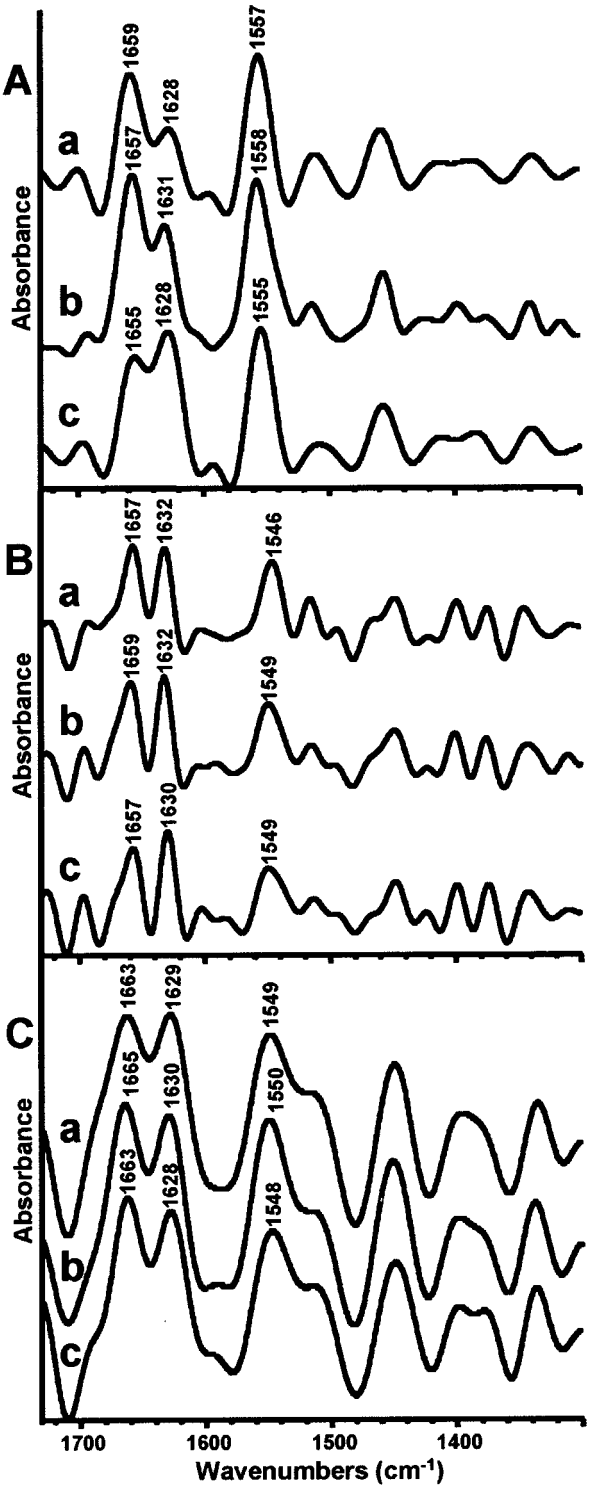

Figure 3. Absorbance peaks of FTIR spectra. **A:** Representative deconvoluted FTIR spectra of type I bovine collagen gels. a, untreated; b, crosslinked with Glut; c, crosslinked with TGA. A shift in the amide I spectral pattern was caused by overnight, 37°C TGA pretreatment, with a reversal of relative peak heights at ~1630 and 1655 cm^{-1}. **B:** Averaged deconvoluted FTIR-RTM spectra of six microscopic cross-sectional areas of porcine aortic valve. a, untreated; b, crosslinked with Glut; c, crosslinked with TGA. A shift in the amide I spectral pattern and slight reversal of the relative peak heights (at ~1630 and 1655 cm^{-1}) was caused by 7-day, 25°C TGA treatment. **C:** Averaged deconvoluted FTIR-RTM spectra of 10 microscopic cross-sectional areas of bovine pericardium. a, untreated; b, crosslinked with Glut; c, crosslinked with TGA. No shift in the spectral pattern is observed in the amide I or amide II regions.

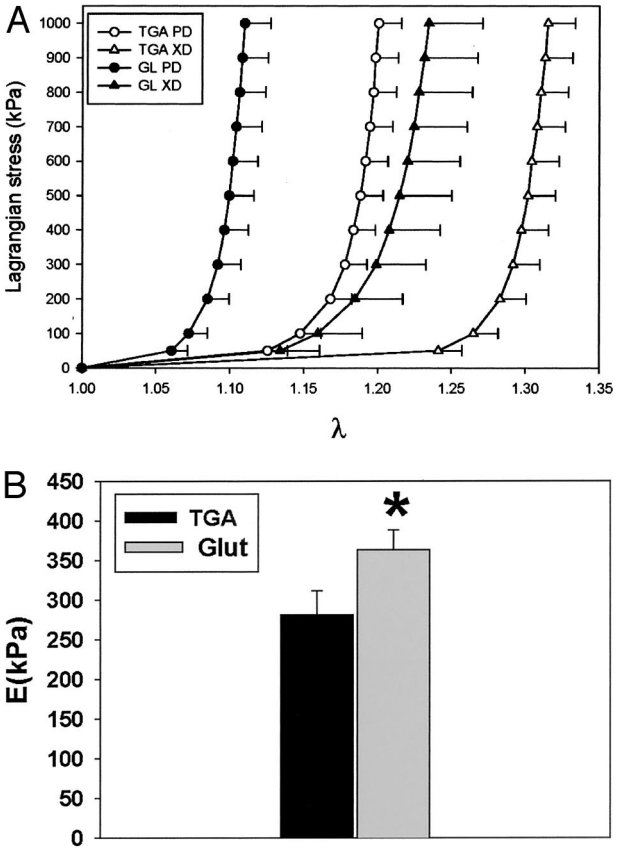

Figure 4. Biomechanical testing of TGA- and Glut-crosslinked pericardium. **A:** The average equi-biaxial stress-strain curves for TGA and Glut specimens, with the error bars indicating 1 SEM ($n = 10$ for TGA and $n = 8$ for Glut). **B:** Mean flexural stiffness results for TGA- and Glut-treated pericardium. GLUT-treated pericardial samples were ~25% stiffer than TGA-treated tissues. *, $P = 0.03$ from the TGA value, and the error bars indicate 1 SEM.

Cell Culture Biocompatibility Studies

SAVICs, A10 cells, and HUVECs were used to investigate the biocompatibility of TGA-crosslinked collagen in comparison to Glut-fixed and noncrosslinked collagen using live/dead assay staining as an endpoint. TGA-crosslinked collagen was highly biocompatible with little cellular death (Figure 5). Neither SAVICs, HUVECs, nor A10 cells cultivated on TGA substrates (Figure 5; b, e, and h, respectively) differed qualitatively from cells cultivated on tissue culture polystyrene (Figure 5; c, f, and i). In contrast, SAVICs cultured on Glut-crosslinked collagen demonstrated greater levels of cell death, and surviving cells cultivated on Glut-pretreated collagen demonstrated bizarre morphologies (fragmented, pyknotic, rounded) (Figure 5; a, d, and g).

SAVICs cultivated on TGA-crosslinked collagen resist calcification in cell culture. SAVICs cultivated on type I collagen (not pretreated with TGA) demonstrated aggregation and macroscopic calcific nodule formation by 72 hours of culture, with progressive severe calcification by 7 days documented by alizarin red staining (Figure 6, A and C). However, SAVICs cultivated on type I collagen pretreated with TGA did not demonstrate nodule formation, nor was there calcification detected by alizarin red staining (Figure 6, B and D). Quantitation of calcium in

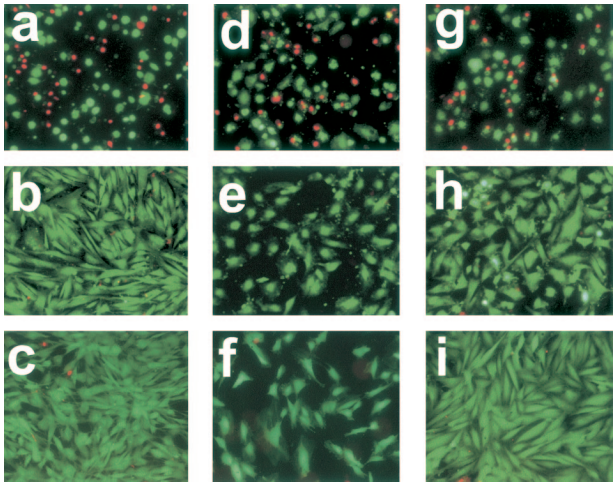

Figure 5. TGA- and Glut-related biocompatability comparison studies. Live-dead assays of three cell lines of SAVICs (**a–c**), HUVECs (**d–f**), and rat arterial smooth muscle cells (A10) (**g–i**), Plated in parallel on either Glut-crosslinked substrate (**a**, **d**, **g**), TGA-crosslinked substrate (**b**, **e**, **h**), or tissue-culture polystyrene (**c**, **f**, **i**). After 24 hours in culture, cells plated on TGA-crosslinked substrate (**b**, **e**, **h**) exhibit higher viability (fluorescent green cells (live) versus fluorescent red cells that are dead) and healthier morphology than those plated on Glut-crosslinked substrate (**a**, **d**, **g**). Cells grown on TGA exhibit similar morphology to those grown on tissue culture plastic (**c**, **f**, **i**). Merged fluorescent micrographs taken using FITC and Texas Red filters. Original magnifications, ×100.

parallel day 7 cultures confirmed this visual observation. Values obtained from replicate experimental set-ups were 1.78 ± 0.13 μmol Ca/mg protein versus 0.84 ± 0.06 μmol Ca/mg protein in SAVICs grown on collagen versus TGA-treated collagen, respectively ($P = 0.013$). It should be noted that Glut-treated collagen substrates were not studied because of their inherent cytotoxicity.

ECM Protein Expression: SAVIC Studies with TGA-Collagen Substrates

To assess the mechanisms responsible for the calcification resistance of TGA-collagen, we investigated the ex-

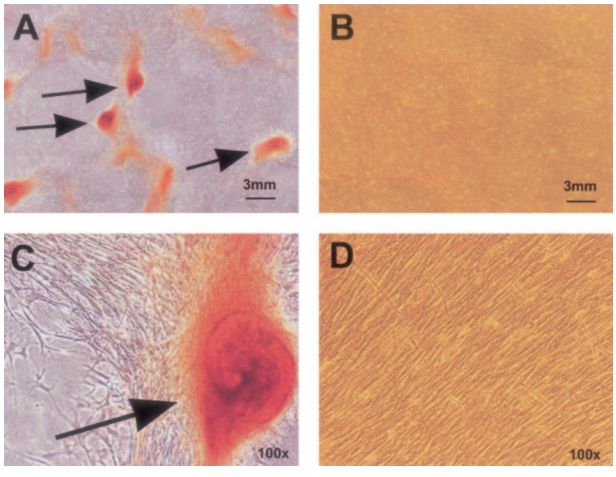

Figure 6. Alizarin red staining of SAVICs after 7 days in culture on untreated type I bovine collagen (**A** and **C**), or on TGA-crosslinked collagen (**B** and **D**). Red stain indicates calcification. Calcific nodules (**arrows**) are macroscopic in size (**A**), while a uniform confluent culture of noncalcified cells is maintained, under the same conditions, but on TGA (**B**). Fields, ×100 (**C** and **D**) show details of cell morphology and staining.

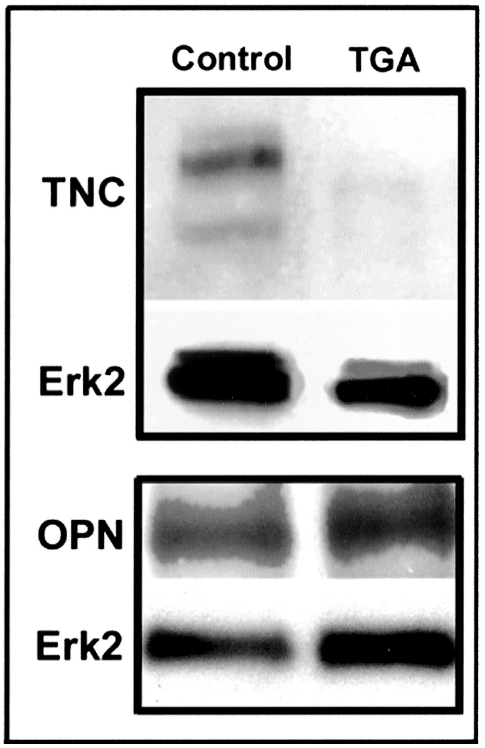

Figure 7. TNC is down-regulated, while OPN is not significantly affected by TGA crosslinking of collagen cell culture substrates. Representative Western blots of cell lysates from 3-day cell cultures of SAVICs on either native type I collagen or on TGA-crosslinked-collagen, with Erk 2 as a loading control marker.

pression of several important ECM proteins in SAVIC cultures using our established model of SAVIC calcification in culture.[17] TNC, an ECM protein demonstrated to be present in human heart valve calcific deposits,[16] was strongly present in SAVICs cultured on noncrosslinked collagen substrates, but was barely detectable in cultures grown on TGA-collagen (Figure 7). However, the levels of OPN, an ECM protein with potent calcification-resistance properties,[20] were not changed in SAVICs cultivated on TGA-collagen (Figure 7) compared to control.

We also investigated the regulation of MMP-9 in SAVICs cultivated on TGA-collagen versus noncrosslinked collagen. Gel zymogram studies showed that calcifying control cultures, grown on noncrosslinked collagen substrates, produced increasing levels of MMP-9 throughout time in conditioned medium, but only when TGF-β1 was added (Figure 8). However, MMP-9 was barely detectable in all of the TGA-collagen SAVIC cultures studied (Figure 8) regardless of the administration of TGF-β1. No such differences were observed in MMP-2 per zymography (Figure 8). The fact that the digestion of collagen substrate per well was significantly greater after 14 days of SAVIC culture on collagen than on TGA-collagen (41.2 $\pm$ 9.8% versus 6.3 $\pm$ 4.3% weight loss, collagen versus collagen-TGA respectively, $P = 0.009$) reflects the importance of MMP-9 and other collagenases in ECM remodeling by valvular interstitial cells. Thus, these studies overall demonstrate profound effects of TGA-crosslinking on ECM-mediated protein expression and calcification related events.

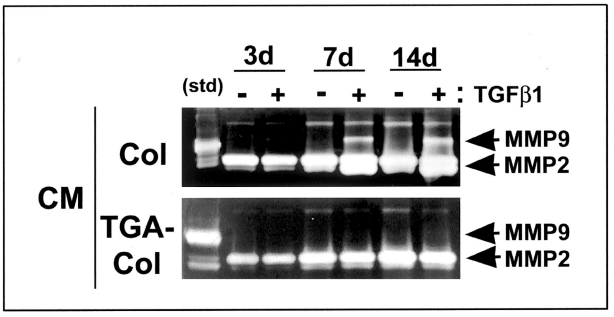

Figure 8. Gel zymography of conditioned medium (CM) from SAVICs cells *in vitro*. Cells were plated on either native collagen (col) or on TGA-crosslinked collagen (TGA-col), in the presence or absence of TGF-β1, and CM harvested at the time points shown. Zymography showed that, unlike cells grown on native collagen, cells grown on TGA-treated substrate secreted no detectable MMP-9 into the CM even in the presence of TGF-β1. MMP-2 secretion did not differ between experimental conditions.

TGA-Crosslinking Inhibits Bioprosthetic Leaflet Calcification: Rat Subdermal Implant Results

TGA-crosslinking effects on calcification *in vivo* were investigated with rat subdermal implant studies of crosslinked (TGA versus Glut) porcine aortic valve cusps and bovine pericardium. Calcium analyses of 21-day explants demonstrated significant inhibition of calcification in both of the TGA-pretreated bioprosthetic materials, compared to the severe mineralization occurring in Glut pretreated explants (Figure 9A, $P < 0.001$). These quantitative results were corroborated by light microscopy studies that showed extensive alizarin red-positive calcifications throughout both the Glut-pretreated porcine aortic valve cusps (Figure 9B, a) and bovine pericardial samples (data not shown). The intrinsic dystrophic calcification observed in the morphology studies (Figure 9B) did not differ from previous results with this model system,[2] and involved primarily the spongiosa layer of the Glut-fixed bioprosthetic heterograft materials (Figure 9B, a); alizarin detectable calcifications were conspicuously absent in the TGA-fixed explants (Figure 9B, b). Routine light microcopy studies revealed that the noncalcified TGA-pretreated implants were not morphologically different from unimplanted specimens (data not shown).

Immunostaining for TNC demonstrated that Glut-pretreated explants were strongly positive for TNC, while TGA-pretreated explants were negative or only weakly positive with staining most apparent in the most superficial regions of the explanted cusps (Figure 9C, b). This difference was statistically significant in histological scoring of TNC staining intensity on a scale of 1 to 5 (21-day Glut versus TGA, 2.9 $\pm$ 0.8 versus 1.4 $\pm$ 0.1; $P = 0.008$). These trends were apparent for both TGA-pretreated porcine aortic valve cusp (Figure 9C, a and b) and bovine pericardium explants (data not shown). Furthermore, MMP-9 immunostaining was significantly weaker in TGA-pretreated explants, which demonstrated only weak peripheral staining, than in Glut-pretreated explants, that showed widespread intense immunostaining (Figure 9C, c and d). Scoring of immunohistochemical intensity on the same scale of 1 to 5 indicated a significant difference in MMP-9 (21-day Glut versus TGA, 4.8 $\pm$ 0.3 versus

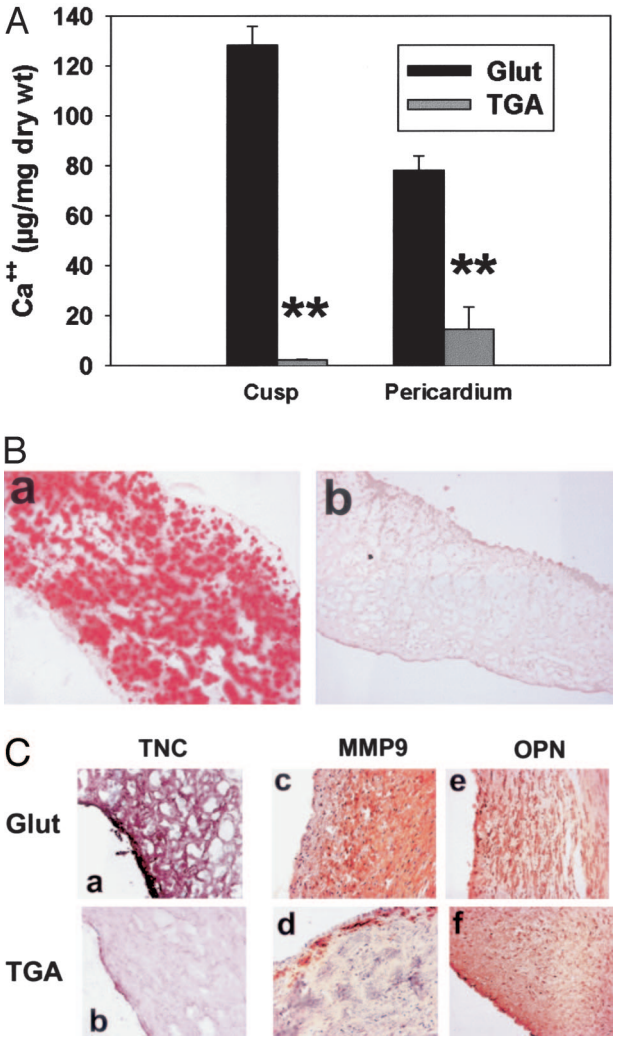

Figure 9. TGA inhibition of rat subdermal implant calcification and ECM protein expression. **A:** Calcium content of 21-day rat subdermal explants, showing reduced calcification in both porcine aortic valve cusp and bovine pericardium treated with TGA versus Glut. **, $P < 0.001$. **B:** Alizarin red staining (for imaging calcium phosphates) of 21-day cusp explants showing a pattern of heavy calcification (red stain) in Glut-treated materials (**a**) versus an absence of alizarin read staining in the TGA-pretreated explants (**b**). **C:** Immunohistochemistry of Glut-pretreated (**a**, **c**, **e**) and TGA-pretreated (**b**, **d**, **f**) 21-day cusp explants for TNC (VIP purple stain) showing lower TNC expression with TGA pretreatment, for MMP-9 (diaminobenzidine brown stain) showing lower expression with TGA pretreatment, and for OPN (diaminobenzidine brown stain) showing no difference between the two groups. Original magnifications: ×100 (**B**); ×200 (**C**, **c–f**); ×400 (**a**, **b**).

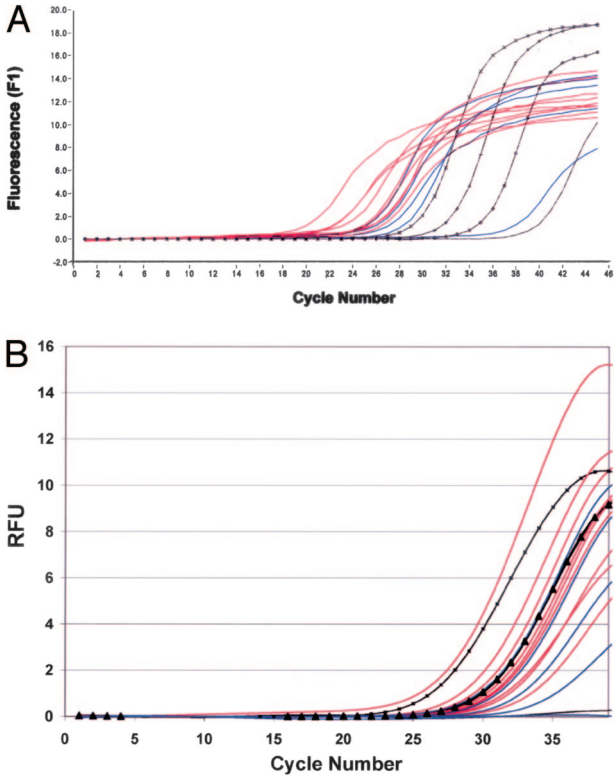

Figure 10. RT-PCR of 21-day rat subdermal explants. Amplification plots of TNC (**A**) and MMP-9 (**B**) from real-time PCR studies for comparison of TGA-pretreated implants (blue) versus Glut-pretreated implants (red) as compared to gene-specific standards. The copy number in each sample was calculated by comparison to the inflection point of each gene-specific copy number standard (**black square**,10^4; **black x**,10^3; **black triangle**,10^2; **black diamond**,10^1; **black line**, negative control). **A:** TNC expression is down-regulated *in vivo* at the mRNA level in TGA-pretreated implants (blue) versus Glut-pretreated implants (red), as demonstrated by the relative inflection points and calculated copy numbers (see text, $P = 0.016$). Parallel RT-PCR analyses for MMP-9 mRNA (**B**) showed a statistically insignificant trend for down-regulation of MMP-9 per mRNA results from TGA-pretreated explants (blue) per real-time PCR results compared to Glut-pretreated explants (red).

2.6 ± 0.3; $P = 0.003$). OPN was strongly present in both the calcified Glut-pretreated bioprosthetic leaflet explants and in the TGA-pretreated explants (Figure 9C, e and f).

TNC mRNA levels were determined in explanted aortic valve extracts (Figure 10A). TNC mRNA expression was significantly higher in Glut explants compared to TGA explants ($6.19 \times 10^5 \pm 4.23 \times 10^5$ versus $1.30 \times 10^4 \pm 1.29 \times 10^4$ transcripts, respectively, as determined from gene-specific copy number standards, $P = 0.016$). RT-PCR analysis for MMP-9 was performed on the same sample sets of aortic valve extracts (Figure 10B). There was considerable variation in MMP-9 transcript number in both groups, with statistically insignificant but higher average copy numbers in Glut explants than in TGA explants ($3.6 \times 10^3 \pm 3.5 \times 10^3$ versus $3.1 \times 10^1 \pm 2.5 \times 10^1$ transcripts, respectively, as determined from external copy number standards).

Discussion

These studies report the synthesis and mechanistic studies of a novel biocompatible polyepoxy crosslinker, TGA, that demonstrates a number of advantages compared to Glut crosslinking of bioprosthetic heart valves. The relative reactivity of epoxides such as TGA with a series of model compounds simulating amino acid functionalities in proteins has been previously published by our group,[21] and revealed the most reactive groups to be sulfur-containing amino acids, with methionine, for example, showing a 20-fold higher reactivity with epoxy than lysine. Thus, the results of both previous and present studies have demonstrated that TGA has broader reactivity than Glut for preparing bioprosthetic leaflet materials in terms of amino acid reactions, and at the same time results in significantly greater collagenase resistance. We

have also demonstrated significant biomechanical compliance advantages using TGA crosslinking compared to Glut. Furthermore, TGA crosslinking promotes resistance to intrinsic bioprosthetic cuspal calcification, which is the most common clinical failure mode of bioprosthetic heart valves.[22,23] The present studies demonstrated anti-calcification activity in 21-day subdermal implants. This implant duration was chosen because a previous clinical pathology study from our group that demonstrated that the level of calcium accumulation seen during this rat implant duration (~120 μg/mg) matched the median level of calcium in bioprosthetic valves that failed because of calcification.[24] Furthermore, anti-calcification efficacy in non-TGA studies by our group in 21-day rat subdermal implants has correlated with inhibition of calcification in 5-month sheep mitral valve replacements.[19]

TGA crosslinking also resulted in a significant change in collagen structure as demonstrated by our FTIR studies of purified type I collagen and of aortic valve cusps, which are principally comprised of collagen; however, bovine pericardium did not demonstrate amide I changes after TGA pretreatment. In particular, the change in the amide I stretching region in porcine aortic cusps is comparable to the same structural change noted in Glut-fixed porcine aortic cusps after ethanol pretreatment, which also confers calcification resistance.[10] It is possible that this change may be masked in pericardium by a more complex noncollagenous protein structure, or that TGA confers resistance to calcification in a manner unrelated to changes in the amide I region. The significant increase in collagenase resistance as a result of TGA fixation is very likely because of changes in collagen structure (as above) resulting from TGA-related chemical reactions that could hypothetically interfere with collagenase-substrate interactions. Previous research from our group has demonstrated that epoxy crosslinking (in contrast to Glut) can involve reactions with not only amino groups, such as the lysine amino side chains in collagen, but sulfur-containing amino acids such as methionine and cysteine.[21] Thus, the crosslinked connective tissue matrix resulting from TGA-amino acid reactions will have a far more complex structure involving collagen-collagen and collagen-protein bonds that would also hypothetically reduce collagenase digestibility.

The biological and ECM mechanisms responsible for TGA's activity both in terms of biocompatibility and calcification resistance are also remarkable. Our cell culture calcification model system is based on SAVICs, because preclinical *in vivo* bioprosthetic valve replacement studies are typically performed in sheep.[10,25] Calcification, TNC, and MMP-9 protein expression were all reduced both in SAVICs grown *in vitro* on TGA-treated collagen and in TGA-pretreated rat subdermal implants, an established *in vivo* model of bioprosthetic calcification.[2,26–30] We have also confirmed TNC expression to be affected by quantitating mRNA using real time PCR. These data indicate that the ECM signaling domains responsible for TNC expression are likely modified by TGA crosslinking. TNC up-regulation in a number of cell types, including arterial smooth muscle cells, has been shown to be β3-integrin-dependent,[31] and thus β3 integrin ligands may be modified or blocked by TGA pretreatment, although other mechanisms may be responsible for the reduction of TNC both in SAVIC cultivated on TGA-crosslinked collagen and in TGA-pretreated rat subdermal explants. Indeed, a positive correlation has been described between TNC expression and MMP activity in both arterial smooth muscle cells and vascular organ cultures.[31,32] Furthermore, both calcification and TNC expression in rat subdermal elastin explants were found to require MMP activity,[18] independent of alkaline phosphatase levels. However, OPN has been found to decrease hydroxyapatite crystal growth[33] and to reduce calcification in cell culture[19] and *in vivo.*[20] Thus, our results suggest that TGA-mediated inhibition of calcification is independent of the level of OPN expression, because OPN was present in both calcified (non-TGA) cell cultures and *in vivo* explants, as well as in the noncalcified TGA samples.

SAVICs cultivated on TGA-pretreated collagen substrates did not calcify or produce detectable (per zymography) MMP-9, even with the administration of TGF-β1, unlike control SAVIC cultures grown on type I collagen substrates that calcified severely, showing enhanced mineralization with the addition of TGF-β1 to the cultures as previously reported.[17] Previous studies have also described the accumulation of TGF-β1 in human calcific valves,[17] a member of the same gene superfamily as the BMPs, and a well-known mineralization inducer in bone and soft tissue. Furthermore, MMPs including MMP-9 cleave LTBP1-bound latent TGF-β1 into the active form,[34] thereby hypothetically promoting a vicious cycle of events whereby interstitial cells are stimulated to produce more MMP-9 by the TGF-β1 that is activated. MMP-9 has been demonstrated by other investigators to be present in clinical explants of both calcified human aortic valves[35,36] and calcified failed bioprosthetic heart valves,[37] and we have immunohistochemically demonstrated its reduced presence in TGA-pretreated rat subdermal explants, compared to increased MMP-9 in calcified Glut-pretreated retrievals. Thus, there is clinical and experimental evidence indicating a mechanistic role for MMP-9 in heart valve calcification that is at this time incompletely understood. The observation that MMP-9 is down-regulated in association with inhibition of calcification in the setting of a TGA-pretreated substrate both *in vitro* and *in vivo* could be of major importance in terms of therapeutic implications.

TGA crosslinking resulted in significant increases in biomechanical compliance compared to Glut pretreatment in our bovine pericardial studies. This implies that the observed resistance of TGA-crosslinked materials to collagenase is not the result of increased binding between the collagen fibrils, but more likely increased masking of the α chain or triple helical structure. Moreover, we observed that TGA-crosslinked bovine pericardium demonstrated stress-strain characteristics (Figure 4A) more similar to those observed by Sacks and Chuong[12] for native bovine pericardium tissues as compared to Glut pretreatment. It can be speculated that these native tissue-like properties result from micromechanical behaviors because of TGA, including an improved ability for collagen fibers to straighten and rotate

under mechanical loading. These results are of interest because they support the hypothesis that TGA-pretreated bioprosthetic heart valves may demonstrate improved durability throughout time compared to Glut-pretreated bioprostheses. Sacks and Schoen[38] have shown in a study of clinical explants that primary material failure of Glut-crosslinked bioprosthetic heart valves can occur in cuspal regions independently of sites of pathological calcification. Their results strongly indicate that improved bioprosthetic heart valve crosslinking formulations that focus only on preventing calcification may not necessarily improve the outcomes of these devices throughout time. However, novel crosslinking strategies, such as the use of TGA, that address both inhibition of calcification and improving important aspects of bioprosthetic cusp biomechanics such as the improved biomechanical compliance because of TGA, may prove to be a more productive and efficacious approach.

It is concluded that TGA pretreatment of collagenous materials, either purified collagen or heterograft biomaterials, is associated with inhibition of dystrophic calcification, both in cell culture and *in vivo*. The mechanisms responsible for this are very likely related to modifications of collagen structure, as well as structural changes in other ECM components, that in turn lead to cellular-ECM interactions resulting in the down-regulation of the expression of calcification-associated ECM proteins including TNC and MMP-9. TGA pretreatment of bioprosthetic heart valve cusps is also associated with improved biocompatibility and biomechanical performance that could hypothetically be of additional therapeutic benefit.

Acknowledgments

We thank Ms. Jennifer LeBold for her assistance in preparing the manuscript and Mr. Zhibin Lu for providing technical assistance.

References

1. Rahimtoola SH: Choice of prosthetic heart valve for adult patients. J Am Coll Cardiol 2003, 41:893–904
2. Levy RJ, Schoen FJ, Levy JT, Nelson AC, Howard SL, Oshry LJ: Biologic determinants of dystrophic calcification and osteocalcin deposition in glutaraldehyde-preserved porcine aortic valve leaflets implanted subcutaneously in rats. Am J Pathol 1983, 113:143–155
3. Schoen FJ, Levy RJ, Nelson AC, Bernhard WF, Nashef A, Hawley M: Onset and progression of experimental bioprosthetic heart valve calcification. Lab Invest 1985, 52:523–532
4. Kim KM, Herrera GA, Battarbee HD: Role of glutaraldehyde in calcification of porcine aortic valve fibroblasts. Am J Pathol 1999, 154: 843–852
5. Dumont CE, Plissonnier D, Guettier C, Michel JB: Effects of glutaraldehyde on experimental arterial iso- and allografts in rats. J Surg Res 1993, 54:61–69
6. Xi T, Ma J, Tian W, Lei X, Long S, Xi B: Prevention of tissue calcification on bioprosthetic heart valve by using epoxy compounds: a study of calcification tests in vitro and in vivo. J Biomed Mater Res 1992, 26:1241–1251
7. Tu R, Shen SH, Lin D, Hata C, Thyagarajan K, Noishiki Y, Quijano RC: Fixation of bioprosthetic tissues with monofunctional and multifunctional polyepoxy compounds. J Biomed Mater Res 1994, 28:677–684
8. Hendriks M, Everaerts F, Verhoeven M: Alternative fixation of bioprostheses. J Long Term Eff Med Implants 2001, 11:163–183
9. Sung HW, Shen SH, Tu R, Lin D, Hata C, Noishiki Y, Tomizawa Y, Quijano RC: Comparison of the cross-linking characteristics of porcine heart valves fixed with glutaraldehyde or epoxy compounds. ASAIO J 1993, 39:M532–M536
10. Vyavahare N, Hirsch D, Lerner E, Baskin JZ, Schoen FJ, Bianco R, Kruth HS, Zand R, Levy RJ: Prevention of bioprosthetic heart valve calcification by ethanol preincubation. Efficacy and mechanisms. Circulation 1997, 95:479–488
11. Eidelman N, Simon JCG: Characterization of combinatorial polymer blend composition gradients by FTIR microspectroscopy. J Res Nat Inst 2004, J Res Natl Inst Stand Technol 2004, 109:219–231
12. Sacks MS, Chuong CJ: Orthotropic mechanical properties of chemically treated bovine pericardium. Ann Biomed Eng 1998, 26:892–902
13. Sun W, Sacks MS, Sellaro TL, Slaughter WS, Scott MJ: Biaxial mechanical response of bioprosthetic heart valve biomaterials to high in-plane shear. J Biomech Eng 2003, 125:372–380
14. Mirnajafi A, Raymer J, Scott MJ, Sacks MS: The effects of collagen fiber orientation on the flexural properties of pericardial heterograft biomaterials. Biomaterials 2004, 26:795–804
15. Gloeckner DC, Billiar KL, Sacks MS: Effects of mechanical fatigue on the bending properties of the porcine bioprosthetic heart valve. ASAIO J 1999, 45:59–63
16. Jian B, Jones PL, Li Q, Mohler III ER, Schoen FJ, Levy RJ: Matrix metalloproteinase-2 is associated with tenascin-C in calcific aortic stenosis. Am J Pathol 2001, 159:321–327
17. Jian B, Narula N, Li QY, Mohler III ER, Levy RJ: Progression of aortic valve stenosis: TGF-beta1 is present in calcified aortic valve cusps and promotes aortic valve interstitial cell calcification via apoptosis. Ann Thorac Surg 2003, 75:456–465
18. Vyavahare N, Jones PL, Tallapragada S, Levy RJ: Inhibition of matrix metalloproteinase activity attenuates tenascin-C production and calcification of implanted purified elastin in rats. Am J Pathol 2000, 157:885–893
19. Wada T, McKee MD, Steitz S, Giachelli CM: Calcification of vascular smooth muscle cell cultures: inhibition by osteopontin. Circ Res 1999, 84:166–178
20. Steitz SA, Speer MY, McKee MD, Liaw L, Almeida M, Yang H, Giachelli CM: Osteopontin inhibits mineral deposition and promotes regression of ectopic calcification. Am J Pathol 2002, 161:2035–2046
21. Alferiev IS, Hinson JT, Ogle M, Breuer E, Levy RJ: High reactivity of alkyl sulfides towards epoxides under conditions of collagen fixation—a convenient approach to 2-amino-4-butyrolactones. Biomaterials 2001, 22:2501–2506
22. Levy RJ: Glutaraldehyde and the calcification mechanism of bioprosthetic heart valves. J Heart Valve Dis 1994, 3:101–104
23. Levy RJ, Schoen FJ, Langer R, Levy JT, Wolfrum J, Hawley MA, Lund SA, Carnes DL: Bioprosthetic heart valve calcification. The Chemistry and Biology of Mineralized Tissues. Edited by WT Butler. Birmingham, EBSCO Media, 1985, pp 375–380
24. Schoen FJ, Kujovich JL, Webb CL, Levy RJ: Chemically determined mineral content of explanted porcine aortic valve bioprostheses: correlation with radiographic assessment of calcification and clinical data. Circulation 1987, 76:1061–1066
25. Schoen FJ, Hirsch D, Bianco RW, Levy RJ: Onset and progression of calcification in porcine aortic bioprosthetic valves implanted as orthotopic mitral valve replacements in juvenile sheep. J Thorac Cardiovasc Surg 1994, 108:880–887
26. Levy RJ, Schoen FJ, Flowers WB, Staelin ST: Initiation of mineralization in bioprosthetic heart valves: studies of alkaline phosphatase activity and its inhibition by AlCl3 or FeCl3 preincubations. J Biomed Mater Res 1991, 25:905–935
27. Bernacca GM, Dimitri WR, Fisher AC, Mackay TG, Wheatley DJ: Chemical modification of bovine pericardium and its effect on calcification in the rat subdermal model. Biomaterials 1992, 13:345–352
28. Vesely I, Noseworthy R, Pringle G: The hybrid xenograft/autograft bioprosthetic heart valve: in vivo evaluation of tissue extraction. Ann Thorac Surg 1995, 60:S359–S364
29. Grabenwoger M, Sider J, Fitzal F, Zelenka C, Windberger U, Grimm M, Moritz A, Bock P, Wolner E: Impact of glutaraldehyde on calcification of pericardial bioprosthetic heart valve material. Ann Thorac Surg 1996, 62:772–777
30. Simionescu DT, Lovekamp JJ, Vyavahare NR: Glycosaminoglycan-degrading enzymes in porcine aortic heart valves: implications for

bioprosthetic heart valve degeneration. J Heart Valve Dis 2003, 12: 217–225
31. Cowan KN, Jones PL, Rabinovitch M: Regression of hypertrophied rat pulmonary arteries in organ culture is associated with suppression of proteolytic activity, inhibition of tenascin-C, and smooth muscle cell apoptosis. Circ Res 1999, 84:1223–1233
32. Cowan KN, Jones PL, Rabinovitch M: Elastase and matrix metalloproteinase inhibitors induce regression, and tenascin-C antisense prevents progression, of vascular disease. J Clin Invest 2000, 105: 21–34
33. Beshensky AM, Wesson JA, Worcester EM, Sorokina EJ, Snyder CJ, Kleinman JG: Effects of urinary macromolecules on hydroxyapatite crystal formation. J Am Soc Nephrol 2001, 12:2108–2116
34. Dallas SL, Rosser JL, Mundy GR, Bonewald LF: Proteolysis of latent transforming growth factor-beta (TGF-beta)-binding protein-1 by osteoclasts. A cellular mechanism for release of TGF-beta from bone matrix. J Biol Chem 2002, 277:21352–21360
35. Satta J, Oiva J, Salo T, Eriksen H, Ohtonen P, Biancari F, Juvonen TS, Soini Y: Evidence for an altered balance between matrix metalloproteinase-9 and its inhibitors in calcific aortic stenosis. Ann Thorac Surg 2003, 76:681–688
36. Edep ME, Shirani J, Wolf P, Brown DL: Matrix metalloproteinase expression in nonrheumatic aortic stenosis. Cardiovasc Pathol 2000, 9:281–286
37. Simionescu A, Simionescu D, Deac R: Biochemical pathways of tissue degeneration in bioprosthetic cardiac valves. The role of matrix metalloproteinases. ASAIO J 1996, 42:M561–M567
38. Sacks MS, Schoen FJ: Collagen fiber disruption occurs independent of calcification in clinically explanted bioprosthetic heart valves. J Biomed Mater Res 2002, 62:359–371